Inhibition of the endocannabinoid system reverses obese phenotype in aged mice and partly restores skeletal muscle function

Lucas Fajardo, Phelipe Sanchez, Jérôme Salles, Jean Paul Rigaudière, Véronique Patrac, Sylvie Caspar-Bauguil, Camille Bergoglgio, Cédric Moro, S. Walrand, Olivier Le Bacquer

Am J Physiol Endocrinol Metab 324: E176–E184, 2023.
First published January 11, 2023; doi:10.1152/ajpendo.00258.2022

american physiological society

AMERICAN JOURNAL OF PHYSIOLOGY
ENDOCRINOLOGY AND METABOLISM

RESEARCH ARTICLE

Inhibition of the endocannabinoid system reverses obese phenotype in aged mice and partly restores skeletal muscle function

Lucas Fajardo,[1] Phelipe Sanchez,[1] Jérôme Salles,[1] Jean Paul Rigaudière,[1] Véronique Patrac,[1] Sylvie Caspar-Bauguil,[2,3] Camille Bergoglgio,[2] Cédric Moro,[2] Stéphane Walrand,[1,4] and Olivier Le Bacquer[1]

[1]*Unité de Nutrition Humaine (UNH), Institut National de la Recherche Agronomique (INRAE), Université Clermont Auvergne, Clermont-Ferrand, France;* [2]*Team MetaDiab, Institute of Metabolic and Cardiovascular Diseases (I2MC), Inserm/Paul Sabatier University UMR1297, Toulouse, France;* [3]*Department of Clinical Biochemistry, Toulouse University Hospitals, Toulouse, France; and* [4]*Service de Nutrition Clinique, Hôpital Gabriel Montpied, Centre Hospitalier Universitaire (CHU) Clermont-Ferrand, Clermont-Ferrand, France*

Abstract

Sarcopenia, the age-related loss of skeletal muscle mass, is associated with lipid accumulation and anabolic resistance; phenomena also observed in obesity and worsen when obesity and aging are combined. The endocannabinoid system (ECS) is overactivated in obesity, but its role in aging obesity-related muscle dysfunction is unknown. The aims of this study were to evaluate the effect of inhibition of the ECS by rimonabant (RIM) on the metabolic alterations induced by a high-fat high-sucrose diet and on skeletal muscle mass/function in aged mice. Eighteen-month-old male mice were subjected to a control (CTL) or a high-fat high-sucrose (HFHS) diet for 24 weeks. Mice were administered with saline or RIM (10 mg/kg/day) for the last 4 weeks of the diet. Skeletal muscle function was evaluated by open-field, rotarod, and grip strength tests. Metabolic alterations in liver, adipose tissue, and skeletal muscle were investigated by quantitative RT-PCR. Body mass was higher in HFHS mice compared to CTL mice (48.0 ± 1.5 vs. 33.5 ± 0.7 g, $P < 0.01$), as a result of fat accumulation (34.8 ± 1.0 vs. 16.7 ± 0.8%, $P < 0.01$). RIM reduced body fat mass in both CTL (−16%, $P < 0.05$) and HFHS conditions (−40%, $P < 0.01$), without affecting hindlimb skeletal muscle mass. In HFHS mice, grip strength evolution was improved (−0.29 ± 0.06 vs. −0.49 ± 0.06 g/g lean mass, $P < 0.05$), and rotarod activity was increased by ≈60% in response to RIM (45.9 ± 6.3 vs. 28.5 ± 4.6 cm, $P < 0.05$). Lipolysis and β-oxidation genes were upregulated in the liver as well as genes involved in adipose tissue browning. These results demonstrate that inhibition of the ECS induces metabolic changes in liver and adipose tissue associated with a reversion of the obese phenotype and that RIM is able to improve motor coordination and muscle strength in aged mice, without affecting skeletal muscle mass.

NEW & NOTEWORTHY In 24-month-old mice submitted to high-fat high-sucrose-induced obesity, inhibition of the endocannabinoid system by rimonabant reversed the obese phenotype by promoting adipose tissue browning and β-oxidation in the liver but not in skeletal muscle. These metabolism modifications are associated with improved skeletal muscle function.

muscle function; obesity; rimonabant; sarcopenia; skeletal muscle

INTRODUCTION

Aging is associated with a gradual loss of physiological functions and functional abilities of the body. The musculoskeletal system is more particularly affected by aging, and its alterations result in a decrease in muscle mass/function, called sarcopenia (1). Therefore, aging is characterized by a reduction in the level of physical activity, which, combined with defects in the use of energy substrates and/or high nutritional intakes, will promote the accumulation of fat mass and ectopic accumulation of lipids in peripheral tissues such as skeletal muscle. This excessive accumulation of fat in response to aging, diet, or obesity combined with sarcopenia is called "sarcopenic obesity" (2) and involves an increased risk of dismobility. The gradual loss of mobility that results from this sarcopenia promotes the development of metabolic syndrome, sedentary lifestyle, and increased risk of falls. Furthermore, a low skeletal muscle mass/strength is a predictor of morbidity and mortality (3, 4). Therefore, prevention of this loss of mobility in aging is critical to maintain physical abilities at an advanced age and to optimize the quality of life of the elderly.

The pathophysiology of sarcopenic obesity is complex and involves alterations in a large number of mechanisms that might explain the reduction of muscle mass and strength. This includes type II muscle fiber atrophy and impaired

Correspondence: O. Le Bacquer (olivier.le-bacquer@inrae.fr).
Submitted 30 September 2022 / Revised 16 December 2022 / Accepted 9 January 2023

control of muscle contraction by the nervous system and thus muscle strength (5–7). Sarcopenia is associated with the appearance of an anabolic resistance associated with a lower response of protein metabolism to the effect of nutrients (amino acids) and hormones (insulin) (8–10). In addition, aging stimulates the infiltration of fat into skeletal muscle, which in turn aggravates the development of sarcopenia (11), and obesity promotes the accumulation of lipids in skeletal muscle, which promotes insulin resistance and muscle wasting (12, 13) and worsens the decrease in strength and muscle performance in aged people (14).

Endocannabinoids (ECs) are defined as endogenous agonists of cannabinoid receptors type 1 and 2 (CB1 and CB2). ECs [such as anandamide and 2-arachidonylglycerol (2-AG)] and EC anabolic and catabolic enzymes and cannabinoid receptors constitute the EC system. The EC system participates in the control of lipid and glucose metabolism at several levels, with the endpoint of the accumulation of energy and fat (15). In the case of excessive nutritional intakes, the EC system becomes overactivated, which contributes to visceral fat accumulation and to the onset of cardiometabolic risk factors that are associated with obesity and type 2 diabetes (15). Accordingly, pharmacological inhibition of CB1 activity with rimonabant has been shown to improve several features of obesity such as overweight, insulin resistance, hyperglycemia, and dyslipidemia both in humans (16, 17) and rodent obese models (18–20) and to normalize adipose tissue metabolism and reverse the development of steatosis in obese mice (21). Besides its role in controlling whole body energy metabolism, several studies also demonstrated the involvement of the EC system in the control of skeletal muscle development and function (22–25). For example, 2-AG levels are reduced during myotube differentiation in vitro, and activation of CB1 by 2-AG prevented myotube formation while increasing myoblast proliferation (22). CB1 antagonism is able to prevent dexamethasone-induced atrophy and to stimulate protein synthesis in vitro in myotubes (23) and to prevent loss of mobility in mdx mice (a model of Duchenne muscular dystrophy) (24). Finally, we documented profound alterations of the EC system and of both circulating and tissue levels of ECs in a rat model of sarcopenia associated with loss of muscle mass and function (25).

The aims of the present study were *1*) to document the metabolic adaptations of peripheral tissues (liver, adipose tissue, and skeletal muscle) after CB1 antagonism in a model of obesity induced by a high-fat high-sucrose diet in old mice, and *2*) to determine whether rimonabant treatment was able to improve skeletal muscle function in this model.

MATERIALS AND METHODS

Animals and Ethical Approval

All experimental protocols were reviewed and approved by the local ethics committee for animal experimentation (CREFA Auvergne, Agreement No. 21250–2019062711554233) and met the National Research Council's *Guidelines for the Care and Use of Laboratory Animals*. Eighteen-month-old C57BL/6 male mice (Elevage Janvier, Le Genest Saint Isle, France) were individually housed in plastic cages and maintained at 21–23°C with a 12:12-h light-dark schedule, given free access to water and food, and followed up to age 24 mo. Mice were fed a normal chow diet (CTL; 25% protein, 61% carbohydrate, 14% fat, and 3.85 kcal/g; Safe-Diets, Augy, France) or a high-fat high-sucrose diet (HFHS; 17% protein, 39.8% carbohydrate, 43.3% fat, and 4.78 kcal/g, INRAE, Jouy en Josas, France) for 22 wk. After 18 wk of diet, mice were maintained on CTL or HSHF diet and received either 10 mg/kg/day of rimonabant or saline solution for 4 wk by oral gavage. Rimonabant solution was extemporaneously prepared in PEG400/Tween80/saline solution (30%/0.5%/69.5%, vol/vol, respectively). For whole body composition analysis, mice were placed in an EchoMRI-100 analyzer (Echo Medical Systems LLC, Houston, TX) to determine fat and lean body mass (g). Euthanasia was performed at 9 AM after overnight fasting during which mice had free access to water. Blood was collected by intracardiac puncture in EDTA-coated tubes. Peripheral tissues (liver, adipose tissue, and skeletal muscle were collected and immediately frozen in liquid nitrogen and stored at −80°C until processing.

Rotarod Test

Motor coordination and performance were assessed by using the accelerating rotarod test. Mice were trained to walk on the rod with constant low-speed rotation (4 rpm) for 3 days with one trial per day (LE-8355, BIOSEB, Vitrolles, France). For the accelerating test (4–40 rpm over 600 s), three trials per test were performed during the test day, with a 20-min interval between trials. The time until the mouse fell from the rod was recorded automatically using the Sedacom software (BIOSEB, Vitrolles, France).

Open Field Test

Open field tests were performed to allow the assessment of the animal's general exploratory locomotion in a novel environment. The open-field apparatus consisted of an arena made with durable material nonabsorbent to the odors (40 cm × 40 cm and 40 cm high) (BIOSEB, Vitrolles, France). The floor of the arena was divided into three zones. The mice were gently placed individually in a corner of the arena and allowed to explore it freely. For each mouse, the locomotor activity was evaluated by measuring total traveled distance (cm), average speed (cm/s), and the duration of activity over a 10-min test period that was recorded using a video tracking camera. SMART Video Tracking software was used to automatically analyze mouse movement. The arena was cleaned with cotton soaked in 70% alcohol between each mouse test.

Handgrip Test

Grip strength was assessed using a commercially available force gauge (BIOSEB, Vitrolles, France) by the same investigator. The apparatus consisted of a metal grid connected to a force transducer. Each mouse was held by the base of its tail and lowered toward the grid of a grip strength meter and allowed to grasp it with its forepaws. The mouse was then pulled steadily away from the rod by its tail until its grip broke. Hindlimb grip strength in each mouse was measured five times.

Plasma Analyses

Overnight fasting insulin level was measured by ELISA (EuroBio, Courtaboeuf, France). Plasma levels of fasting

glucose, triglycerides, nonesterified fatty acids (NEFA), and cholesterol were determined using a Konelab 20 analyzer (Thermo-Electron Corporation).

Determination of Triacylglycerol, Diacylglycerol, and Ceramide Content in Muscle Tissue

Triacylglycerol, diacylglycerol, and ceramide species content was determined by high-performance liquid chromatography-mass spectrometry after lipid extraction as described elsewhere (26).

RNA Extraction and Quantitative Real-Time PCR

Total RNA was extracted using Trizol reagent (Invitrogen) according to the manufacturer's instructions. RNA was quantified by measuring optical density at 260 nm. The concentrations of the mRNAs corresponding to genes of interest were measured by reverse transcription followed by real-time PCR using a Rotor-Gene Q (Qiagen) system. One microgram of total RNA was reverse transcribed using SuperScript III reverse transcriptase and a combination of random hexamer and oligo-dT primers (Invitrogen). PCR amplification was performed in a 20 μL total reaction volume. The real-time-PCR mixture contained 5 μL of diluted cDNA template, 10 μL of 2× Rotor-Gene SYBR Green PCR master mix, and 0.5 μM of forward and reverse primers. The amplification profile was initiated by 5 min incubation at 95°C to activate HotStarTaq Plus DNA Polymerase, followed by 40 cycles of two steps: 95°C for 5 s (denaturation step) and 60°C for 10 s (annealing/extension step). Relative mRNA concentrations were analyzed using Rotor-Gene software. The relative abundance of mRNAs was calculated using the $2^{-\Delta\Delta CT}$ method with 18S as a housekeeping gene. The primers used in the PCR are described in Table 1.

Statistical Analyses

Data are expressed as mean ± SE. Differences between groups were analyzed with a two-way ANOVA. Post hoc comparisons were conducted with Tukey's test. Statistical significance was set at $P < 0.05$ for all analyses.

RESULTS

Body and Organ Weights

Baseline body weights of the different groups of mice were comparable. After 18 wk of diets, the average body weight of HFHS animals was increased by ≈35% compared with CTL (47.4 ± 1.1 vs. 35.0 ± 0.5 g, $P < 0.01$, Fig. 1*A*). This gain in body weight was mainly attributable to a ≈300% increase in body fat mass in HFHS mice (16.7 ± 0.8 vs. 5.9 ± 0.4 g, $P < 0.01$) and a slight ≈10% increase in body lean mass (30.9 ± 0.4 vs. 28.5 ± 0.2 g, $P < 0.01$). From *week 18* to *week 22*, in response to rimonabant treatment, HFHS mice lost significantly more body weight than HFHS mice receiving saline solution (−9.5 ± 1.3 vs. −3.7 ± 1.5 g, $P < 0.01$, Fig. 1*B*). This loss of body weight in response to rimonabant was also observed in CTL mice (−1.4 ± 0.4 vs. −0.3 ± 0.6 g, $P < 0.01$, Fig. 1*B*). This loss of body weight was reflected in fat mass, which was significantly decreased in HFHS mice treated with rimonabant compared to mice treated with saline. Indeed, while the saline HFHS group had a nonsignificant fat mass loss of approximately ≈20% (presaline, 16.3 ± 1.1 g vs. postsaline, 12.5 ± 1.2 g), the rimonabant HFHS group had a significant decrease in body fat mass with an almost 50% loss of body fat mass (prerimonabant, 17.2 ± 1.1 g vs. postrimonabant, 8.5 ± 1.1 g, $P < 0.01$). While food intake was not affected in CTL mice in response to rimonabant, we observed a transiently decreased food intake in the HFHS + RIM mice as compared to HFHS mice (Fig. 1*C*). Consistent with the loss of body mass, the weight of gonadal and subcutaneous white adipose tissues was reduced in rimonabant-treated CTL mice (approximately equal to −20%, $P = 0.08$) and significantly reduced in rimonabant-treated HFHS mice compare to HFHS mice (Table 2). Analysis of the hindlimb muscles revealed significant decreases in gastrocnemius, tibialis, and quadriceps weight in rimonabant-treated CTL mice and in the soleus of rimonabant-treated HFHS mice compared to untreated mice (Table 2). Skeletal muscle diacylglycerol, ceramide, and sphingomyelin levels were unaffected and triacylglycerol significantly increased in response to the HFHS diet. Diacyglycerol, triacylglycerol, and ceramide levels were not affected by RIM treatment (Table 3).

Table 1. *Primer list for real-time quantitative PCR*

Gene Name	5′-Sense Primer-3′	5′-Antisense Primer-3′
ACC1	ACCTGGTGGAGTGGCTGGAG	ATGGCGACTTCTGGGTTGGC
Atrogin/MAFBx	AAGCTTGTGCGATGTTACCCA	CACGGATGGTCAGTGCCCTT
CPT1a	GATGACGGCTATGGTGTTTCCTAC	TCCCAAAGCGGTGTGAGTCTG
CPT1b	TGGGACTGGTCGATTGCATC	TCAGGGTTTGTCGGAAGAAGAA
FAT/CD36	TTGTACCTATACTGTGGCTAAATGAGA	CTTGTGTTTTGAACATTTCTGCTT
FATP	TTCTCGGAGTCTGGAATGCT	CACAGAGGCTGTTCCTGCTC
HSL	GTTACCACCCTGCAGTCCTC	AATGGTCCTCTGCCTCTGTC
MCAD	TTTCGGAGGCTATGGATTCAACAC	TCAATGTGCTCACGAGCTATGATC
MuRF1	AGGTGTCAGCGCAAAGCAGT	CCTCCTTTGTCCTCTTGCTG
PEPCK	CCCGAAGGCAAGAAGAAATA	CGTTTTCTGGGTTGATAGCC
PGC1α	GAAGTGGTGTAGCGACCAATC	AATGAGGGCAATCCGTCTTCA
PPARγ	CAAGAATACCAAAGTGCGATCAA	GAGCTGGGTCTTTTCAGAATAATAAG
PRDM16	CAGCACGGTGAAGCCATTC	GCGTGCATCCGCTTGTG
18S	CGGCTACCACATCCAAGGAA	GCTGGAATTACCGCGGCT

ACC1, acetyl-CoA carboxylase 1; CPT1, carnitine palmitoyltransferase 1; FAT/CD36, fatty acid transport/CD36; HSL, hormone-sensitive lipase; MCAD, medium-chain acyl-CoA dehydrogenase; MuRF1, muscle ring finger 1; PEPCK, phosphoenolpyruvate carboxykinase; PGC1α, peroxisome proliferator-activated receptor-γ coactivator-1α; PPAR-γ, peroxisome proliferator-activated receptor-γ; PRDM16, PR domain containing 16.

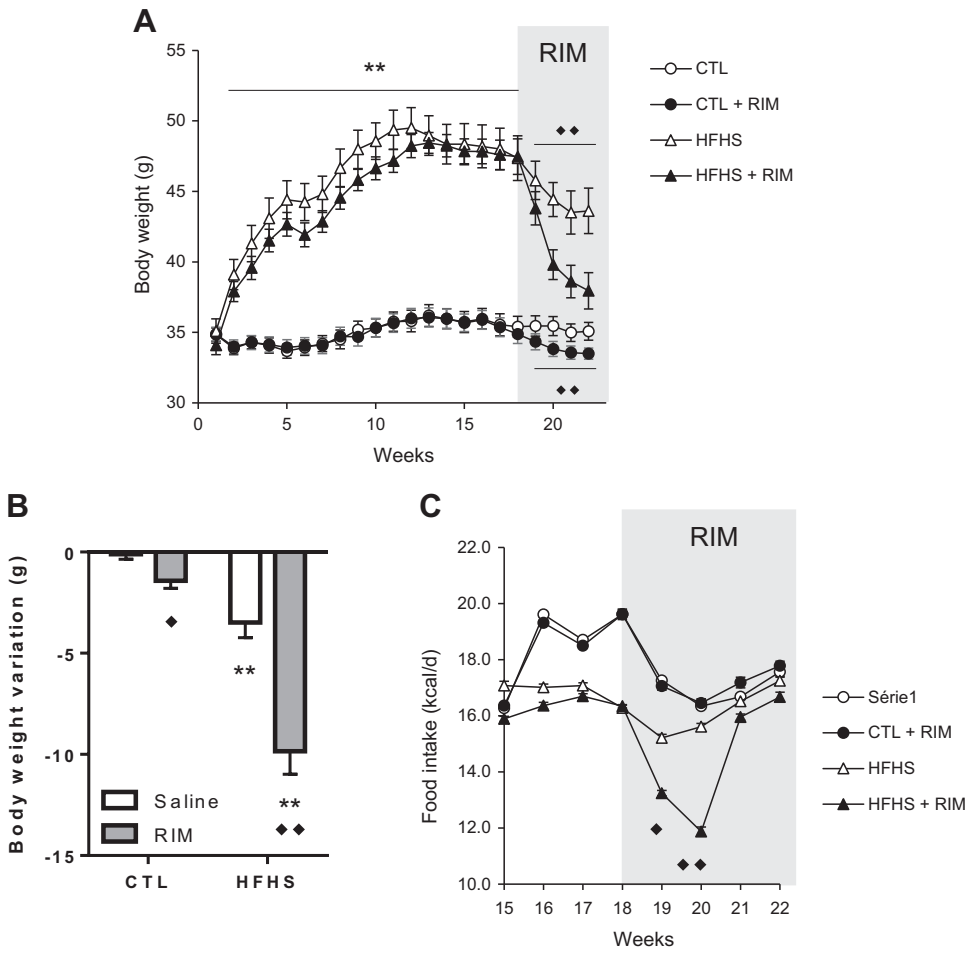

Figure 1. Body weight is reduced in response to a 4-week oral treatment with rimonabant. *A*: body weight in response to a high-fat high-sucrose diet (HFHS) diet and rimonabant treatment. *B*: body weight variation in response to 4-week rimonabant treatment. *C*: daily food intake. *P* values were assessed by two-way ANOVA. Bonferroni posttests were used to compare replicate means by row. $^{**}P < 0.01$ vs. CTL; ♦$P < 0.05$, ♦♦$P < 0.01$ vs. saline.

Serum Parameters

At the end of the experiment, fasted blood glucose levels were similar in all diet and treatment groups. Insulin levels were twice as high in response to the HFHS diet (Table 4). Rimonabant treatment leads to a ≈40% and ≈45% reduction in insulin levels in CTL and HFHS mice, respectively (Table 4). Cholesterol and NEFA blood levels were both increased in HFHS mice compared to CTL mice, while triglyceride levels were unchanged (Table 4). Cholesterol, NEFA, and triglyceride levels were unaffected by rimonabant in the CTL mice. However, this treatment increased cholesterol and reduced triglyceride and NEFA levels in HFHS mice (Table 4).

Muscle Function Tests

To evaluate motor coordination, mice were subjected to the rotarod test. Rotarod performance was reduced by ≈30% in response to the HFHS diet (Fig. 2*A*). We also observed a decreased performance on the rotarod test for all the groups of mice tested between the start and the end of the rimonabant/saline treatment (Fig. 2, *A* and *B*). At the end of the

Table 2. *Hindlimb skeletal muscle and tissue weight in mice submitted to HFHS diet and rimonabant*

	CTL + SAL	CTL + RIM	HFHS + SAL	HFHS + RIM
Body weight, g	33.6 ± 0.6	31.9 ± 0.5	41.7 ± 1.6**	36.2 ± 1.4$$
Gastrocnemius, mg	125.0 ± 2.7	115.9 ± 3.0$	120.2 ± 3.2	117.4 ± 2.8
EDL, mg	11.1 ± 0.4	10.4 ± 0.4	10.1 ± 0.4*	9.6 ± 0.4*
Soleus, mg	9.5 ± 0.4	9.0 ± 0.4	9.2 ± 0.3	8.3 ± 0.3$
Tibialis, mg	49.7 ± 0.8	45.0 ± 0.9$$	47.9 ± 1.2	46.7 ± 1.4
Quadriceps, mg	179.6 ± 8.0	165.3 ± 5.9$	176.6 ± 11.4	161.9 ± 7.6
GWAT, mg	453 ± 49	348 ± 30	811 ± 85**	524 ± 77$$
SWAT, mg	189 ± 21	149 ± 12	659 ± 84**	441 ± 84**$$
Liver, g	1.32 ± 0.04	1.34 ± 0.11	1.69 ± 0.08**	1.50 ± 0.07$

Results are expressed as means ± SE. Mice were 24 months old. CTL, control; SAL, saline; RIM, rimonaban; EDL, extensor digitorum longus; GWAT and SWAT, gonadal white adipose tissue and subcutaneous white adipose tissue. *P* values were assessed by two-way ANOVA. Bonferroni posttests were used to compare replicate means by row. $^{*}P < 0.05$, $^{**}P < 0.01$ vs. high-fat high-sucrose diet (HFHS) vs. control (CTL); $$P < 0.05$, $$$P < 0.01$ rimonabant vs. saline.

Table 3. *Skeletal muscle lipid accumulation in response to HFHS and rimonabant treatment*

	CTL + SAL	CTL + RIM	HFHS + SAL	HFHS + RIM
Diacylglycerols, μg/mg wet tissue	0.20 ± 0.03	0.25 ± 0.05	0.29 ± 0.05	0.28 ± 0.05
Triacylglycerols, μg/mg wet tissue	8.2 ± 1.6	9.2 ± 1.5	13.8 ± 2.1**	14.5 ± 1.9**
Ceramides, nmol/g wet tissue	8.1 ± 1.3	12.2 ± 3.5	7.4 ± 1.0	8.7 ± 1.4
Sphyngomyelins, nmol/g wet tissue	32.8 ± 5.4	42.4 ± 7.5	28.3 ± 4.8	38.1 ± 6.0

Results are expressed as means ± SE. Mice were 24 months old. SAL, saline; RIM, rimonabant. *P* values were assessed by two-way ANOVA. Bonferroni posttests were used to compare replicate means by row. $^{**}P < 0.01$, high-fat high-sucrose diet (HFHS) vs. control (CTL).

treatment, rotarod performance was unaffected by rimonabant in CTL mice [63.4 ± 6.4 vs. 53.4 ± 5.7 s, not significant (NS)] but was ameliorated in HFHS mice (28.5 ± 64.6 vs. 45.9 ± 6.3 s, $P < 0.05$). To assess the strength of mice in response to the HFHS diet and rimonabant treatment, mice were subjected to a grip strength test before the start (*week 18*) and at the end (*week 22*) of the rimonabant treatment. As shown in Fig. 2*C*, between the beginning and end of treatment, the loss of grip strength corrected to the amount of lean body mass in CTL and HFHS mice was similar (−0.62 ± 0.09 vs. −0.49 ± 0.06 g/g lean body, NS). In response to rimonabant, the decrease in grip strength was reduced by ≈25% in CTL mice (−0.46 ± 0.10 vs. −0.62 ± 0.09 g/g lean body; $P < 0.1$) and by ≈40% in HFHS mice (−0.29 ± 0.06 vs. −0.49 ± 0.10 g/g lean body; $P < 0.05$). To evaluate voluntary activity, mice were subjected to the open field test. Distance traveled during the test was decreased in HFHS mice compare to CTL mice, and unaffected by rimonabant treatment in CTL and HFHS mice (Fig. 2*D*). Average gait speed was not affected by the HFHS diet compared with the CTL diet, nor by treatment with rimonabant (data not shown).

Gene Expression in Adipose Tissue

To investigate the effect of the HFHS diet and rimonabant treatment on adipose tissue, the mRNA expression of genes involved in the transport of fatty acids [fatty acid transport (FAT)/CD36] and their mobilization for use [hormone-sensitive lipase (HSL)] was measured by RT-qPCR in perirenal adipose tissue. The fate of fatty acids was also studied by studying genes involved in β-oxidation [medium-chain acyl-CoA dehydrogenase (MCAD) and carnitine palmitoyltransferase 1a (CPT1a)] and thermogenesis [peroxisome proliferator-activated receptor-γ coactivator-1α (PGC1α) and PR domain containing 16 (PRDM16)]. FAT/CD36 expression was increased twofold in response to HFHS, and rimonabant treatment increased its expression in both CTL and HFHS mice (Table 5). HSL mRNA expression was unaltered in response to HFHS but significantly increased in CTL + RIM and HFHS + RIM conditions (Table 5). CPT1b and MCAD mRNA expression was unaltered by the HFHS diet. However, CPT1b and MCAD mRNA levels were increased in response to rimonabant in both CTL and HFHS mice (Table 5). PGC1α and PRDM16 mRNA expression was unaffected in response to HFHS, but PGC1α mRNA expression was twofold higher in response to rimonabant in CTL and HFHS mice (Table 5), and PRDM16 mRNA levels were twofold and threefold higher in response to rimonabant in CTL and HFHS mice, respectively (Table 5).

Table 4. *Metabolic parameters in mice submitted to HFHS diet and rimonabant*

	CTL + SAL	CTL + RIM	HFHS + SAL	HFHS + RIM
Insulin, ng/mL	0.71 ± 0.33	0.28 ± 0.05$	1.76 ± 0.32*	1.00 ± 0.37*$
Glucose, g/L	2.08 ± 0.06	1.94 ± 0.08	1.87 ± 0.22	2.00 ± 0.21
Cholesterol, g/L	0.89 ± 0.03	0.91 ± 0.02	1.47 ± 0.21**	1.76 ± 0.16**
Triglycerides, g/L	0.58 ± 0.07	0.57 ± 0.05	0.59 ± 0.06	0.44 ± 0.02*$
NEFA, mg/L	142.7 ± 14.1	141.9 ± 18.9	196.8 ± 19.7*	164.9 ± 11.2$

Results are expressed as means ± SE. Mice were 24 months old. SAL, saline; RIM, rimonabant; NEFA, nonesterified fatty acid. *P* values were assessed by two-way ANOVA. Bonferroni posttests were used to compare replicate means by row. $^{*}P < 0.05$, $^{**}P < 0.01$, high-fat high-sucrose diet (HFHS) vs. control (CTL); $\$P < 0.05$, rimonabant vs. saline.

Gene Expression in Liver

To assess the effect of the HFHS diet and rimonabant on carbohydrate and lipid metabolism in the liver, the mRNA expression of genes involved in β-oxidation (MCAD and CPT1a), lipogenesis and triglyceride synthesis [peroxisome proliferator-activated receptor-γ (PPAR-γ) and acetyl-CoA carboxylase 1 (ACC1)], and gluconeogenesis [phosphoenolpyruvate carboxykinase (PEPCK)] was measured by RT-qPCR. CPT1a mRNA expression was increased in response to HFHS. Its expression level was unaffected in response to rimonabant in CTL mice but was significantly increased in HFHS + RIM mice (Table 5). MCAD mRNA expression was unaffected by rimonabant in CTL mice, and the slight increase observed in response to HFHS was exacerbated by rimonabant in HFHS + RIM mice (Table 5). ACC1 mRNA expression and PPARγ mRNA expression were both increased by HFHS and unaffected by rimonabant whatever the diet was (Table 5). Finally, PEPCK mRNA expression was unaffected by rimonabant in the CTL condition. Its increased expression level in HFHS was partly reversed by rimonabant in HFHS + RIM mice (Table 5).

Gene Expression in Skeletal Muscle

We analyzed by RT-qPCR the effect of rimonabant on the mRNA levels of genes involved in fatty acid transport (FATP and FAT/CD36), β-oxidation (MCAD and CPT1b), and proteolysis [muscle ring finger 1 (MuRF1) and Atrogin/MAFBx] in gastrocnemius. Compared to CTL diet, the HFHS diet induced a ≈50% increase in FATP expression ($P < 0.01$) and a doubling of FAT/CD36 expression ($P < 0.01$), without rimonabant altering this expression (Table 5). This increase in fatty acid transport gene expression was accompanied in HFHS mice by a ≈50% increase in MCAD expression ($P < 0.05$) and a doubling of CPT1b mRNA expression ($P < 0.01$). Again, rimonabant treatment

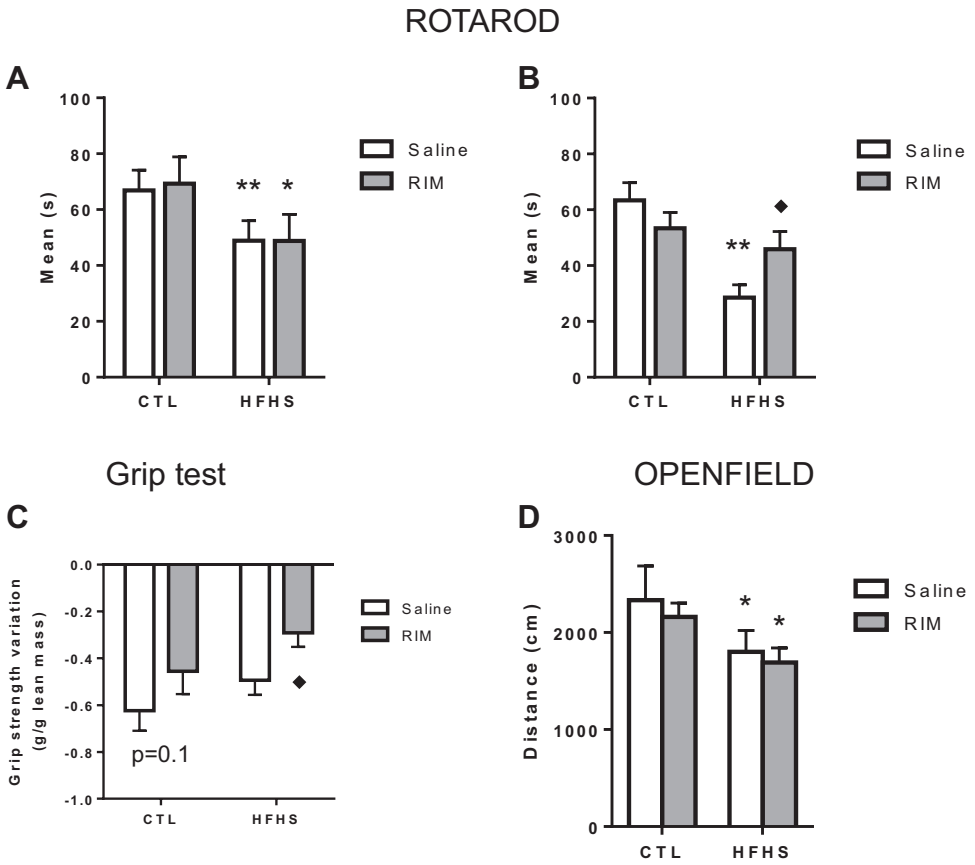

Figure 2. Effect of rimonabant on locomotor activity and strength. *A* and *B*: muscle coordination measured using rotarod before (*A*) and after (*B*) 4-week oral rimonabant treatment. *C*: variation in grip strength between the beginning and the end of the 4-week oral rimonabant treatment. *D*: voluntary locomotor activity measured using open field. *P* values were assessed by two-way ANOVA. Bonferroni posttests were used to compare replicate means by row. $*P < 0.05$, $**P < 0.01$ vs. CTL; ♦$P < 0.05$ vs. saline.

did not alter the expression of these mRNAs in either CTL or HFHS conditions (Table 5). The HFHS diet induced a significant increase in the expressions of both MurF1 and Atrogin/MAFBx ($P < 0.05$), which were not altered by the rimonabant treatment (Table 5).

DISCUSSION

The objective of this study was to investigate whether a treatment with rimonabant (CB1 antagonist) was able to correct the obese phenotype in a context of high-fat high-sucrose diet-induced obesity in aged mice and to determine whether CB1 antagonism was able to improve skeletal muscle mass and/or function in this model. We provide evidence that rimonabant induces metabolic adaptations (e.g., insulinemia) and molecular changes in liver and adipose tissue associated with a reversion of the obese phenotype. We also demonstrated that rimonabant was able to improve skeletal muscle function in old obese and sarcopenic mice.

We observed that rimonabant strongly reduced the obesity phenotype in old mice submitted to the HFHS diet. This is in agreement with previous works conducted in HFD-diet adult rodents showing that the rimonabant antiobesity effect was associated with a normalization of adipocyte and liver metabolisms and by increased β-oxidation (20, 21, 27, 28). Reduction of adipose mass by rimonabant resulted from enhanced lipolysis through the liver induction of enzymes of the β-oxidation (27, 29). In the present study, we observed that the evolution of CPT1 and MCAD mRNA expression levels (β-oxidation major regulators) in response to the HFHS diet and rimonabant treatment was tissue-dependent. In the liver, the HFHS diet increased the expression of CPT1a. Rimonabant further increased its expression and increased the expression of MCAD mRNA. These data are in agreement with those observed by Flamment et al. (29) showing that rimonabant treatment leads to an improvement of hepatic mitochondrial function by increasing substrate oxidation and fatty acid entry into mitochondria for the β-oxidation pathway. In adipose tissue, CPT1b and MCAD mRNA levels were unchanged in response to the HFHS diet but were increased in response to rimonabant. In terms of energy production, the importance of adipose tissue β-oxidation is very limited compared to that occurring in liver and skeletal muscle. However, it is known that fatty acid oxidation is required for the maintenance of the brown adipocyte phenotype and thermogenic programming (30), which can concur with the reduction of obesity by increasing energy expenditure. The increased expression of PGC1α and PRDM16 (adipose tissue browning markers) in response to rimonabant we documented in adipose tissue support this hypothesis. In this regard, the increased FAT/CD36 expression in response to rimonabant may promote the entry of fatty acids into the adipocyte for the β-oxidation to support adipose tissue browning and thermogenesis. Finally, expression of CPT1b and MCAD mRNA was increased by the HFHS diet in skeletal muscle, but rimonabant failed to modify these expressions. In rat L6 myotubes in culture, a recent study demonstrated that for rimonabant to increase muscle

Table 5. *Real-time PCR quantification in adipose tissue, liver, and skeletal muscle*

	CTL + SAL	CTL + RIM	HFHS + SAL	HFHS + RIM
Adipose tissue				
FAT/CD36	3.68 ± 0.79	6.23 ± 1.85$	10.17 ± 2.60**	22.00 ± 8.97**$
HSL	4.66 ± 0.88	8.12 ± 1.88$	5.14 ± 0.82	11.45 ± 3.81$
CPT1b	2.42 ± 0.77	4.51 ± 1.48$	1.69 ± 0.69	6.75 ± 2.38$
MCAD	3.59 ± 1.03	6.07 ± 1.40$	4.17 ± 1.08	13.82 ± 4.72$$
PGC1α	1.54 ± 0.49	2.80 ± 0.67$	0.97 ± 0.30	2.23 ± 0.72$
PRDM16	4.34 ± 1.00	8.17 ± 1.84$	5.55 ± 0.90	15.14 ± 3.45$
Liver				
CPT1a	0.54 ± 0.04	0.59 ± 0.03	1.37 ± 0.18**	2.19 ± 0.41**$
MCAD	0.71 ± 0.07	0.72 ± 0.05	0.93 ± 0.27	1.50 ± 0.23$ (P = 0.07)
ACC1	0.77 ± 0.09	0.79 ± 0.11	1.07 ± 0.13*	1.04 ± 0.08*
PPARγ	0.58 ± 0.05	0.59 ± 0.05	2.09 ± 0.49**	1.69 ± 0.37*
PEPCK	1.48 ± 0.10	1.73 ± 0.12	2.85 ± 0.46**	2.04 ± 0.3$ (P = 0.08)
Skeletal muscle				
FATP	0.79 ± 0.08	0.76 ± 0.07	1.45 ± 0.15**	1.66 ± 0.18**
FAT/CD36	0.97 ± 0.10	1.04 ± 0.05	2.28 ± 0.27**	2.15 ± 0.29**
CPT1b	2.57 ± 0.15	2.34 ± 0.17	4.93 ± 0.56**	4.90 ± 0.64**
MCAD	1.05 ± 0.06	1.02 ± 0.04	1.71 ± 0.15*	1.59 ± 0.13*
MURF1	1.00 ± 0.06	0.97 ± 0.05	1.38 ± 0.30*	1.52 ± 0.25*
Atrogin	0.85 ± 0.11	0.83 ± 0.16	1.58 ± 0.41*	1.54 ± 0.37*

Mice were 24 months old. Results are expressed as mean arbitrary units ± SE. Results of RT-PCR quantification in adipose tissue {fatty acid transport [FAT/CD36; hormone-sensitive lipase (HSL)], β-oxidation [carnitine palmitoyltransferase 1b (CPT1b) and medium-chain acyl-CoA dehydrogenase (MCAD)], adipose tissue browning [peroxisome proliferator-activated receptor-γ coactivator-1α, (αPGC1α) and PR domain containing 16 (PRDM16)], liver (β-oxidation CPT1a and MCAD), lipid metabolism [acetyl-CoA carboxylase 1 (ACC1), and peroxisome proliferator-activated receptor-γ (PPARγ)], and carbohydrate metabolism [phosphoenolpyruvate carboxykinase (PEPCK)]} and skeletal muscle {fatty acid transport (FATP and FAT/CD36), β-oxidation (CPT1b and MCAD), and proteolysis [muscle ring finger 1 (MURF1) and atrogin]}. SAL, saline; RIM, rimonabant. P values were assessed by 2-way ANOVA. Bonferroni posttests were used to compare replicate means by row *$P < 0.05$, **$P < 0.01$ vs. high-fat high-sucrose diet (HFHS) vs. control (CTL); $$P < 0.05$, $$$P < 0.01$ rimonabant vs. saline.

β-oxidation, glucose transporter Glut4 has to be overexpressed (31). The fact that obesity is known to reduce Glut4 expression in skeletal muscle (32) might have prevented rimonabant from further increased CPT1b and MCAD mRNA expression and β-oxidation as observed in the liver. Altogether, these data demonstrate that, in old mice, the rimonabant-induced reduction of obesity is mainly attributable to an increased fatty acid β-oxidation in the liver and to increased energy expenditure through browning of the adipose tissue.

Sarcopenia, the loss of muscle mass and function associated with aging, is closely associated with physical disabilities (1). Furthermore, a higher rate of functional decline has been reported in subjects with sarcopenic obesity, where obesity and sarcopenia coexist (2, 33). In the present study, we observed a slight reduction in skeletal muscle mass, yet not significant, in response to HFHS. As such, our model cannot be described as a model of sarcopenic obesity but rather as a model of obesity in aged mice. Sarcopenic obesity is not a function of age but rather results from the severity of several factors, including inflammation, insulin resistance, and skeletal muscle lipotoxicity. It is possible that in our study the level of obesity achieved or its duration was not sufficient to induce a level of insulin resistance, inflammation, or lipotoxicity severe enough to exacerbate the age-associated loss of skeletal muscle mass. However, our analysis of skeletal muscle function revealed that the HFHS diet altered motor coordination and performance, exploratory locomotion, and strength in aged mice. Rimonabant was able to partly prevent this loss of motor coordination in the HFHS mice. Similarly, the loss of grip strength was ameliorated in response to rimonabant in both CTL and HFHS mice. Such a positive effect of rimonabant on skeletal muscle function has been previously documented in mdx mice (a model of Duchenne muscular dystrophy) (24).

How rimonabant improves skeletal muscle function in our model of sarcopenic obesity is unclear. Obesity is correlated to a reduction of muscle mass, impaired muscle repair, and increased fibrosis, which impairs muscle function by reducing motile and contractile functions (34). The regenerative potential of skeletal muscle relies on satellite cells and fibro/adipogenic progenitors (FAP) (35). In conditions of chronic low-grade inflammation, such as observed in aging and obesity, satellite cells and FAP functions are impaired leading to poor skeletal muscle regeneration and fibrosis (35). Several studies demonstrated that the inactivation of CB1 exerts potent antifibrotic effects in inflammation-driven models of fibrosis (36–38). Further studies will be required to determine whether the effect of rimonabant on the maintenance of muscle function was associated with an antifibrotic effect. The effect of rimonabant on the maintenance of muscle performance in sarcopenic obesity may also result from effects on skeletal muscle contraction. Indeed, endocannabinoids acutely modulate contraction strength in skeletal muscle, through different mechanisms including the regulation of neuromuscular transmission or the efficiency of excitation-contraction coupling (39). For example, CB1 agonists such as 2-AG and AEA reduced the acetylcholine release at the presynaptic motor nerve terminal, a prerequisite for muscle contraction, and the depolarization-induced release of Ca^{2+} from the sarcoplasmic reticulum of the muscle fiber (40–42). This suggests that obesity-associated overactivity of the endocannabinoid system could induce such deleterious effects on muscle contraction and that CB1 antagonist (e.g.,

rimonabant) could improve it. To our knowledge, no studies attempted to characterize the effect of rimonabant on these muscle parameters.

DATA AVAILABILITY

Data will be made available upon reasonable request.

ACKNOWLEDGMENTS

We thank all the staff from the Unité d'Expérimentation en Nutrition (INRA Clermont-Ferrand-Theix, France) for excellent assistance with animal care. We are also grateful to Marine Araujo for the technical support with muscle lipid analyses.

GRANTS

This study was supported by the French government IDEX-ISITE Initiative 16-IDEX-0001 (CAP 20–25) and I-SITE project (CAP 2025) of the University of Clermont Auvergne.

DISCLOSURES

No conflicts of interest, financial or otherwise, are declared by the authors.

AUTHOR CONTRIBUTIONS

O.L.B. and J.S. conceived and designed research; L.F., P.S., J.P.R., V.P., S.C.-B., and C.B. performed experiments; L.F., O.L.B., J.S. and C.M. analyzed data; O.L.B., J.S., C.M., and S.W. interpreted results of experiments; L.F., P.S., J.P.R., V.P., S.C.-B, and C.B. prepared figures; L.F. and O.L.B. drafted manuscript; O.L.B., J.S., C.M., and S.W. edited and revised manuscript; L.F., O.L.B., P.S., J.S., J.P.R., V.P., S.C.-B., C.B., C.M., and S.W. approved final version of manuscript.

REFERENCES

1. **Cruz-Jentoft AJ**, **Sayer AA.** Sarcopenia. *Lancet* 393: 2636–2646, 2019 [Erratum in *Lancet* 393: 2590, 2019]. doi:10.1016/S0140-6736(19)31138-9.
2. **Zamboni M**, **Mazzali G**, **Fantin F**, **Rossi A**, **Di Francesco V.** Sarcopenic obesity: a new category of obesity in the elderly. *Nutr Metab Cardiovasc Dis* 18: 388–395, 2008. doi:10.1016/j.numecd.2007.10.002.
3. **Studenski S**, **Perera S**, **Patel K**, **Rosano C**, **Faulkner K**, **Inzitari M**, **Brach J**, **Chandler J**, **Cawthon P**, **Connor EB**, **Nevitt M**, **Visser M**, **Kritchevsky S**, **Badinelli S**, **Harris T**, **Newman AB**, **Cauley J**, **Ferrucci L**, **Guralnik J.** Gait speed and survival in older adults. *JAMA* 305: 50–58, 2011. doi:10.1001/jama.2010.1923.
4. **Szulc P**, **Munoz F**, **Marchand F**, **Chapurlat R**, **Delmas PD.** Rapid loss of appendicular skeletal muscle mass is associated with higher all-cause mortality in older men: the prospective MINOS study. *Am J Clin Nutr* 91: 1227–1236, 2010. doi:10.3945/ajcn.2009.28256.
5. **Nilwik R**, **Snijders T**, **Leenders M**, **Groen BB**, **van Kranenburg J**, **Verdijk LB**, **van Loon LJ.** The decline in skeletal muscle mass with aging is mainly attributed to a reduction in type II muscle fiber size. *Exp Gerontol* 48: 492–498, 2013. doi:10.1016/j.exger.2013.02.012.
6. **Delbono O.** Neural control of aging skeletal muscle. *Aging Cell* 2: 21–29, 2003. doi:10.1046/j.1474-9728.2003.00011.x.
7. **Larsson L**, **Degens H**, **Li M**, **Salviati L**, **Lee YI**, **Thompson W**, **Kirkland JL**, **Sandri M.** Sarcopenia: aging-related loss of muscle mass and function. *Physiol Rev* 99: 427–511, 2019. doi:10.1152/physrev.00061.2017.
8. **Haran PH**, **Rivas DA**, **Fielding RA.** Role and potential mechanisms of anabolic resistance in sarcopenia. *J Cachexia Sarcopenia Muscle* 3: 157–162, 2012. doi:10.1007/s13539-012-0068-4.
9. **Cuthbertson D**, **Smith K**, **Babraj J**, **Leese G**, **Waddell T**, **Atherton P**, **Wackerhage H**, **Taylor PM**, **Rennie MJ.** Anabolic signaling deficits underlie amino acid resistance of wasting, aging muscle. *FASEB J* 19: 1–22, 2005. doi:10.1096/fj.04-2370com.
10. **Volpi E**, **Mittendorfer B**, **Rasmussen BB**, **Wolfe RR.** The response of muscle protein anabolism to combined hyperaminoacidemia and glucose-induced hyperinsulinemia is impaired in the elderly. *J Clin Endocrinol Metab* 85: 4481–4490, 2000. doi:10.1210/jcem.85.12.7021.
11. **Visser M**, **Goodpaster BH**, **Kritchevsky SB**, **Newman AB**, **Nevitt M**, **Rubin SM**, **Simonsick EM**, **Harris TB.** Muscle mass, muscle strength, and muscle fat infiltration as predictors of incident mobility limitations in well-functioning older persons. *J Gerontol A Biol Sci Med Sci* 60: 324–333, 2005. doi:10.1093/gerona/60.3.324.
12. **Tardif N**, **Salles J**, **Guillet C**, **Tordjman J**, **Reggio S**, **Landrier JF**, **Giraudet C**, **Patrac V**, **Bertrand-Michel J**, **Migne C**, **Collin ML**, **Chardigny JM**, **Boirie Y**, **Walrand S.** Muscle ectopic fat deposition contributes to anabolic resistance in obese sarcopenic old rats through eIF2alpha activation. *Aging cell* 13: 1001–1011, 2014. doi:10.1111/acel.12263.
13. **Masgrau A**, **Mishellany-Dutour A**, **Murakami H**, **Beaufrere AM**, **Walrand S**, **Giraudet C**, **Migne C**, **Gerbaix M**, **Metz L**, **Courteix D**, **Guillet C**, **Boirie Y.** Time-course changes of muscle protein synthesis associated with obesity-induced lipotoxicity. *J Physiol* 590: 5199–5210, 2012. doi:10.1113/jphysiol.2012.238576.
14. **Delmonico MJ**, **Harris TB**, **Visser M**, **Park SW**, **Conroy MB**, **Velasquez-Mieyer P**, **Boudreau R**, **Manini TM**, **Nevitt M**, **Newman AB**, **Goodpaster BH**, **Health, Aging, and Body.** Longitudinal study of muscle strength, quality, and adipose tissue infiltration. *Am J Clin Nutr* 90: 1579–1585, 2009. doi:10.3945/ajcn.2009.28047.
15. **Mazier W**, **Saucisse N**, **Gatta-Cherifi B**, **Cota D.** The endocannabinoid system: pivotal orchestrator of obesity and metabolic disease. *Trends Endocrinol Metab* 26: 524–537, 2015. doi:10.1016/j.tem.2015.07.007.
16. **Van Gaal L**, **Pi-Sunyer X**, **Després J-P**, **McCarthy C**, **Scheen A.** Efficacy and safety of rimonabant for improvement of multiple cardiometabolic risk factors in overweight/obese patients: pooled 1-year data from the Rimonabant in Obesity (RIO) program. *Diabetes Care* 31: S229–S240, 2008. doi:10.2337/dc08-s258.
17. **Despres JP**, **Golay A**, **Sjostrom L**, **Rimonabant in Obesity-Lipids Study Groupl.** Effects of rimonabant on metabolic risk factors in overweight patients with dyslipidemia. *New Engl J Med* 353: 2121–2134, 2005. doi:10.1056/NEJMoa044537.
18. **Gary-Bobo M**, **Elachouri G**, **Gallas JF**, **Janiak P**, **Marini P**, **Ravinet-Trillou C**, **Chabbert M**, **Cruccioli N**, **Pfersdorff C**, **Roque C**, **Arnone M**, **Croci T**, **Soubrie P**, **Oury-Donat F**, **Maffrand JP**, **Scatton B**, **Lacheretz F**, **Le Fur G**, **Herbert JM**, **Bensaid M.** Rimonabant reduces obesity-associated hepatic steatosis and features of metabolic syndrome in obese Zucker fa/fa rats. *Hepatology* 46: 122–129, 2007. doi:10.1002/hep.21641.
19. **Poirier B**, **Bidouard JP**, **Cadrouvele C**, **Marniquet X**, **Staels B**, **O'Connor SE**, **Janiak P**, **Herbert JM.** The anti-obesity effect of rimonabant is associated with an improved serum lipid profile. *Diabetes Obes Metab* 7: 65–72, 2005. doi:10.1111/j.1463-1326.2004.00374.x.
20. **Jbilo O**, **Ravinet-Trillou C**, **Arnone M**, **Buisson I**, **Bribes E**, **Peleraux A**, **Penarier G**, **Soubrie PL**, **Fur G**, **Galiegue S**, **Casellas P.** The CB1 receptor antagonist rimonabant reverses the diet-induced obesity phenotype through the regulation of lipolysis and energy balance. *FASEB J* 19: 1567–1569, 2005. doi:10.1096/fj.04-3177fje.
21. **Jourdan T**, **Djaouti L**, **Demizieux L**, **Gresti J**, **Verges B**, **Degrace P.** CB1 antagonism exerts specific molecular effects on visceral and subcutaneous fat and reverses liver steatosis in diet-induced obese mice. *Diabetes* 59: 926–934, 2010. doi:10.2337/db09-1482.
22. **Iannotti FA**, **Silvestri C**, **Mazzarella E**, **Martella A**, **Calvigioni D**, **Piscitelli F**, **Ambrosino P**, **Petrosino S**, **Czifra G**, **Biro T**, **Harkany T**, **Taglialatela M**, **Di Marzo V.** The endocannabinoid 2-AG controls skeletal muscle cell differentiation via CB1 receptor-dependent inhibition of Kv7 channels. *Proc Natl Acad Sci U S A* 111: E2472–E2481, 2014. doi:10.1073/pnas.1406728111.
23. **Le Bacquer O**, **Lanchais K**, **Combe K**, **Van Den Berghe L**, **Walrand S.** Acute rimonabant treatment promotes protein synthesis in C2C12 myotubes through a CB1-independent mechanism. *J Cell Physiol* 236: 2669–2683, 2021. doi:10.1002/jcp.30034.

24. **Iannotti FA**, **Pagano E**, **Guardiola O**, **Adinolfi S**, **Saccone V**, **Consalvi S**, **Piscitelli F**, **Gazzerro E**, **Busetto G**, **Carrella D**, **Capasso R**, **Puri PL**, **Minchiotti G**, **Marzo DV.** Genetic and pharmacological regulation of the endocannabinoid CB1 receptor in Duchenne muscular dystrophy. *Nat Comm* 9: 3950, 2018. doi:10.1038/s41467-018-06267-1.
25. **Le Bacquer O**, **Salles J**, **Piscitelli F**, **Sanchez P**, **Martin V**, **Montaurier CD**, **Marzo V**, **Walrand S.** Alterations of the endocannabinoid system and circulating and peripheral tissue levels of endocannabinoids in sarcopenic rats. *J Cachexia Sarcopenia Muscle* 13: 662–676, 2022. doi:10.1002/jcsm.12855.
26. **Bacquer Combe LO**, **Montaurier K**, **Salles J C**, **Giraudet C**, **Patrac V**, **Domingues-Faria C**, **Guillet C**, **Louche K**, **Boirie Y**, **Sonenberg N**, **Moro C**, **Walrand S.** Muscle metabolic alterations induced by genetic ablation of 4E-BP1 and 4E-BP2 in response to diet-induced obesity. *Mol Nutr Food Res* 61: 1700128, 2017. doi:10.1002/mnfr.201700128.
27. **Watanabe T**, **Kubota N**, **Ohsugi M**, **Kubota T**, **Takamoto I**, **Iwabu M**, **Awazawa M**, **Katsuyama H**, **Hasegawa C**, **Tokuyama K**, **Moroi M**, **Sugi K**, **Yamauchi T**, **Noda T**, **Nagai R**, **Terauchi Y**, **Tobe K**, **Ueki K**, **Kadowaki T.** Rimonabant ameliorates insulin resistance via both adiponectin-dependent and adiponectin-independent pathways. *J Biol Chem* 284: 1803–1812, 2009. doi:10.1074/jbc.M807120200.
28. **Backhouse K**, **Sarac I**, **Shojaee-Moradie F**, **Stolinski M**, **Robertson MD**, **Frost GS**, **Bell JD**, **Thomas EL**, **Wright J**, **Russell-Jones D**, **Umpleby AM.** Fatty acid flux and oxidation are increased by rimonabant in obese women. *Metabolism* 61: 1220–1223, 2012 [Erratum in *Metabolism* 63: e7, 2014]. doi:10.1016/j.metabol.2012.02.012.
29. **Flamment M**, **Gueguen N**, **Wetterwald C**, **Simard G**, **Malthiery Y**, **Ducluzeau PH.** Effects of the cannabinoid CB1 antagonist rimonabant on hepatic mitochondrial function in rats fed a high-fat diet. *Am J Physiol Endocrinol Metab* 297: E1162–E1170, 2009. doi:10.1152/ajpendo.00169.2009.
30. **Gonzalez-Hurtado E**, **Lee J**, **Choi J**, **Wolfgang MJ.** Fatty acid oxidation is required for active and quiescent brown adipose tissue maintenance and thermogenic programing. *Mol Metab* 7: 45–56, 2018. doi:10.1016/j.molmet.2017.11.004.
31. **Muller GA**, **Wied S**, **Herling AW.** Analysis of direct effects of the CB1 receptor antagonist rimonabant on fatty acid oxidation and glycogenolysis in liver and muscle cells in vitro. *Biochemistry (Mosc)* 84: 954–962, 2019. doi:10.1134/S000629791908011X.
32. **Kahn BB**, **Pedersen O.** Suppression of GLUT4 expression in skeletal muscle of rats that are obese from high fat feeding but not from high carbohydrate feeding or genetic obesity. *Endocrinology* 132: 13–22, 1993. doi:10.1210/endo.132.1.8419118.
33. **Chang CI**, **Huang KC**, **Chan DC**, **Wu CH**, **Lin CC**, **Hsiung CA**, **Hsu CC**, **Chen CY.** The impacts of sarcopenia and obesity on physical performance in the elderly. *Obes Res Clin Pract* 9: 256–265, 2015. doi:10.1016/j.orcp.2014.08.003.
34. **Akhmedov D**, **Berdeaux R.** The effects of obesity on skeletal muscle regeneration. *Front Physiol* 4: 371, 2013. doi:10.3389/fphys.2013.00371.
35. **Collao N**, **Farup J**, **De Lisio M.** Role of metabolic stress and exercise in regulating fibro/adipogenic progenitors. *Front Cell Dev Biol* 8: 9, 2020. doi:10.3389/fcell.2020.00009.
36. **Marquart S**, **Zerr P**, **Akhmetshina A**, **Palumbo K**, **Reich N**, **Tomcik M**, **Horn A**, **Dees C**, **Engel M**, **Zwerina J**, **Distler O**, **Schett G**, **Distler JH.** Inactivation of the cannabinoid receptor CB1 prevents leukocyte infiltration and experimental fibrosis. *Arthritis Rheum* 62: 3467–3476, 2010. doi:10.1002/art.27642.
37. **Teixeira-Clerc F**, **Julien B**, **Grenard P**, **Tran Van Nhieu J**, **Deveaux V**, **Li L**, **Serriere-Lanneau V**, **Ledent C**, **Mallat A**, **Lotersztajn S.** CB1 cannabinoid receptor antagonism: a new strategy for the treatment of liver fibrosis. *Nat Med* 12: 671–676, 2006. doi:10.1038/nm1421.
38. **Rezq S**, **Hassan R**, **Mahmoud MF.** Rimonabant ameliorates hepatic ischemia/reperfusion injury in rats: Involvement of autophagy via modulating ERK- and PI3K/AKT-mTOR pathways. *Int Immunopharmacol* 100: 108140, 2021. doi:10.1016/j.intimp.2021.108140.
39. **Ge D**, **Odierna GL**, **Phillips WD.** Influence of cannabinoids upon nerve-evoked skeletal muscle contraction. *Neurosci Lett* 725: 134900, 2020. doi:10.1016/j.neulet.2020.134900.
40. **Oz M**, **Tchugunova Y**, **Dinc M.** Differential effects of endogenous and synthetic cannabinoids on voltage-dependent calcium fluxes in rabbit T-tubule membranes: comparison with fatty acids. *Eur J Pharmacol* 502: 47–58, 2004. doi:10.1016/j.ejphar.2004.08.052.
41. **Oz M**, **Tchugunova YB**, **Dunn SM.** Endogenous cannabinoid anandamide directly inhibits voltage-dependent Ca(2+) fluxes in rabbit T-tubule membranes. *Eur J Pharmacol* 404: 13–20, 2000. doi:10.1016/S0014-2999(00)00396-4.
42. **Morsch M**, **Protti DA**, **Cheng D**, **Braet F**, **Chung RS**, **Reddel SW**, **Phillips WD.** Cannabinoid-induced increase of quantal size and enhanced neuromuscular transmission. *Sci Rep* 8: 4685, 2018. doi:10.1038/s41598-018-22888-4.